Kinetics of CheA Autophosphorylation and Dephosphorylation Reactions†

Paul Tawa and Richard C. Stewart*

Department of Microbiology and Immunology, McGill University, Montreal, Quebec H3A 2B4, Canada

Received February 23, 1994; Revised Manuscript Received April 19, 1994®

ABSTRACT: The protein kinase CheA of *Escherichia coli* plays a central role in the signal transduction pathway controlling the swimming behavior of the cell in response to extracellular chemical gradients. CheA autophosphorylates at a rate controlled by the ligand binding state of chemotaxis receptor/transducer proteins. CheA directs the activities of CheY and CheB, effector proteins that become phosphorylated as a result of their interaction with phospho-CheA. In this study, we performed a detailed kinetic analysis of CheA's autophosphorylation reaction, and its dephosphorylation by ADP. Our kinetic data are consistent with a three-step mechanism for CheA autophosphorylation/dephosphorylation involving (i) substrate binding, (ii) phospho-transfer, and (iii) product release. We determined the dissociation constant for the kinetically defined CheA·ATP complex to be approximately 300 μM and the limiting rate constant for autophosphorylation to be approximately 0.026 s^{-1} at saturating ATP concentration. Our results indicate that the apparent dissociation constant of the phospho-CheA·ADP complex is approximately 42 μM and that the limiting rate constant for CheA dephosphorylation is approximately 0.028 s^{-1} at saturating ADP concentration. We corroborated the kinetically determined K_d values by performing independent ligand binding experiments. In addition, we found that the kinetics of trans-phosphorylation, involving mutant proteins CheA48HQ and CheA470GK, exhibited kinetic properties similar to those observed for autophosphorylation of wild-type CheA, although the limiting rate constant (0.008 s^{-1}) was somewhat slower for this trans-phosphorylation reaction. These results will provide a framework for assessing the effects of various *cheA* mutations as well as for exploring the nature of CheA regulation by the chemotaxis receptor/transducer proteins.

CheA is a cytoplasmic protein kinase that plays a central role in the signal transduction pathway that enables chemotaxis in *Escherichia coli* [reviewed in Stewart and Dahlquist (1987), Bourret et al. (1991), and Parkinson (1993)]. In the presence of ATP and Mg^{2+}, CheA readily autophosphorylates at histidine-48 (Hess et al., 1987, 1988a). Hess et al. (1987) demonstrated that this reaction is readily reversible as phospho-CheA will phosphorylate ADP. Results of *in vitro* experiments indicate that CheA's autokinase activity is regulated by inner-membrane-spanning methyl-accepting chemotaxis receptors (MCPs) such that CheA's autokinase activity is affected when the cell experiences concentration changes of chemical stimuli present in its environment (Borkovich et al., 1989; Borkovich & Simon, 1990; Ninfa et al., 1991). This MCP-mediated modulation activity is dependent on the presence of the coupling factor CheW, a cytoplasmic protein required for assembly of an MCP/CheW/CheA ternary complex (Gegner et al., 1992; Schuster et al., 1993).

Once phosphorylated, CheA's phosphoryl group is rapidly targeted to CheY or CheB, chemotaxis proteins that affect cell swimming behavior (Hess et al., 1988b; Wylie et al., 1988). When repellant stimuli are encountered, MCPs are thought to transmit signals that augment CheA's autokinase activity, resulting in increased levels of phospho-CheY and phospho-CheB. Phospho-CheY interacts directly with the flagellar switch to promote clockwise flagellar rotation, resulting in cellular tumbles and redirection of the swimming cell (Bourret et al., 1990; Barak & Eisenbach, 1992; Roman et al., 1992). Phospho-CheB has elevated methylesterase activity and proceeds to demethylate the MCPs, leading to attenuation of MCP signaling, a process involved in sensory adaptation in the chemotaxis system (Lupas & Stock, 1989; Stewart et al., 1990).

The molecular nature of MCP regulation of CheA autokinase activity has not yet been elucidated. However, *in vitro* studies have provided some insight into the biochemical mechanism of communication between MCPs and CheA. CheA's *in vitro* autophosphorylating activity is dramatically increased when both MCPs and CheW are provided; this enhancement can be negated by addition of an appropriate chemoattractant (Borkovich et al., 1989; Borkovich & Simon, 1990; Ninfa et al., 1991; Gegner et al., 1992). CheW is required for this activation by acting as a coupling factor that enables formation of an MCP/CheW/CheA ternary complex in which CheA kinase activity is linked to the signaling state of the MCP (Gegner & Dahlquist, 1991; Liu & Parkinson, 1991; Gegner et al., 1992). Although CheW alone does not affect CheA activity *in vitro*, CheA/CheW complexes immunoprecipitated from cell lysates exhibit enhanced autokinase activity resulting from an apparent increased affinity for ATP (McNally & Matsumura, 1991). Together, these *in vitro* results suggest that activation of CheA by MCPs and CheW occurs by switching CheA from a relatively dormant state to one that is highly active.

As a first step toward understanding the mechanism of CheA's autophosphorylation reaction, its regulation by the chemotaxis system, and the effects of various *cheA* mutations, we undertook a detailed kinetic characterization of CheA's interactions with ATP and ADP in the absence of the regulators

† This work was supported by a grant from the Canadian Medical Research Council (MT10826) and by Establishment Grant 900129 from Le Fonds de la Recherches en Santé du Québec. R.C.S. is supported by an MRC Scholarship.

* To whom correspondence should be addressed at the Department of Microbiology and Immunology, McGill University, 3775 University St., Montreal, Quebec H3A 2B4, Canada. Telephone: 514-398-4667. FAX: 514-398-7052. Email: CYRS@MUSICA.McGill.CA.

® Abstract published in *Advance ACS Abstracts*, June 1, 1994.

0006-2960/94/0433-7917$04.50/0

CheW and MCP. We have developed a minimal kinetic scheme to account for our experimental observations. Such analysis enabled us to quantify the affinity of CheA for ATP, of phospho-CheA for ADP, and of the limiting rate constants for the phosphorylation and dephosphorylation reactions. These results should prove useful in future investigations exploring the nature of CheA's activation by the chemotaxis receptors.

MATERIALS AND METHODS

Bacterial Strains and Plasmids. *Escherichia coli* strain RP3098 [Δ(*flhA-flhD*); kindly provided by J. S. Parkinson, University of Utah] is a K12 derivative which expresses no chemotaxis proteins and was used in purifying CheA. The overexpression plasmid pAR1:cheA (Wolfe & Stewart, 1993) contains *cheA* under control of the *tac* promoter, the $lacI^Q$ gene to enable isopropyl β-D-thiogalactopyranoside (IPTG) inducible expression of *cheA*, and the ampicillin-resistance gene.

Protein Purification. CheA was purified as described (Wolfe & Stewart, 1993) and stored at −80 °C in buffer containing 10% glycerol. Purified CheA was greater than 95% pure as judged by Coomassie Blue staining, and its identity was verified by Western blotting using affinity-purified anti-CheA IgG. Protein concentrations were determined using the bicinchoninic acid assay (Pierce) using BSA as a protein standard. [^{32}P]Phospho-CheA was generated and isolated as described (Hess et al., 1988) with the omission of glycerol during the procedure for the reasons described below.

CheA Phosphorylation Assays. All reactions were performed at 25 °C in TKMD buffer (50 mM Tris-HCl/50 mM KCl/5 mM $MgCl_2$/0.5 mM dithiothreitol, pH 7.5). Glycerol was found to have significant effects on the affinity of CheA for ATP and was thus removed (by dialysis) from CheA samples prior to initiation of reactions. CheA activity was not affected by storage of samples in this buffer at −20 °C for periods of 6 months. Autophosphorylation reactions contained 2 μM CheA and were initiated by the addition of [γ-^{32}P]ATP (~5000 cpm/pmol) at the indicated concentrations. For trans-phosphorylation reactions involving CheA48HQ and CheA470GK, each protein was present at a final concentration of 2 μM, and the protein mixtures were allowed to preequilibrate at room temperature for 60 min prior to addition of ATP to allow heterodimer formation. At the appropriate time points, aliquots were removed, and the reaction was quenched by addition of 2 × SDS/PAGE sample buffer. Samples were subject to SDS/PAGE in a Bio-Rad minigel apparatus using the Chromaphor protein visualization system (Promega). Immediately following electrophoresis, CheA bands were excised, and the level of phosphorylation was quantified by liquid scintillation counting using BioLite cocktail (ICN) and a Beckman LS6800 counter. Background counts (i.e., obtained in the absence of CheA) were less than 5% of the counts observed at the earliest time point at each ATP concentration.

Dephosphorylation reactions contained 1 μM [^{32}P]phospho-CheA (~2500 cpm/pmol) and were initiated by the addition of the appropriate amount of ADP and otherwise performed and analyzed as for the autophosphorylation reactions.

Steady-state CheA autophosphorylation kinetics were measured using a coupled ATPase assay system (Norby, 1988) as described by Ninfa et al. (1991) and Lukat et al. (1991) at varying ATP concentrations. CheA was present at a concentration of 1 μM. The reactions also included 10 μM CheY, 1 μM CheZ, 1 mM phosphoenolpyruvate (PEP), 0.2 mM NADH, 10 units/mL pyruvate kinase (PK), and 30 units/mL lactate dehydrogenase (LDH) (Sigma). These reagents enabled monitoring of the rate of ATP consumption by measuring spectrophotometrically the rate of oxidation of NADH to NAD^+ ($\epsilon_{NADH \rightarrow NAD^+} = 0.0062\ \mu M^{-1}cm^{-1}$). Each reaction was initiated by addition of the appropriate concentration of ATP, and the rate of NADH oxidation was measured continuously using the timedrive analysis feature of a Perkin Elmer Lambda 2 UV/VIS spectrometer. The concentrations of CheY, CheZ, PK, and LDH were varied without noticing any appreciable effect on the rates of the reactions, indicating that CheA autophosphorylation was rate-limiting under these conditions.

To measure the stoichiometry of CheA phosphorylation, 2.5-μL aliquots of 200 μM CheA were added to a 0.5-mL preequilibrated mixture containing 2 mM ATP, 1 mM PEP, 0.2 mM NADH, 10 units/mL PK, and 30 units/mL LDH, and the subsequent decrease in A_{340} was measured in a dual-beam spectrophotometer. The reference cuvette was treated identically except that the 2.5-μL aliquots added contained buffer only and lacked CheA. The radioisotope labeling assay to measure phosphorylation stoichiometry was performed by allowing reactions containing 2 μM CheA and 2 mM [γ-^{32}P]-ATP to reach equilibrium and then terminating the reactions by spotting aliquots onto 1-cm nitrocellulose squares. The squares were allowed to dry, followed by four washes in 100 mL of TBS (20 mM Tris-HCl/0.5 M NaCl, pH 7.5) to remove inorganic phosphate, dried, and analyzed by scintillation counting. To determine background levels of radioactivity, similar reactions were conducted using CheA48HQ (a CheA mutant lacking the site of autophosphorylation) instead of wild-type CheA.

Phosphate exchange reactions between phospho-CheA and ATP were performed with 2 μM [^{32}P]phospho-CheA and were initiated by the addition of unlabeled ATP to give a final concentration of 1 mM. Time points were collected by spotting aliquots of the reactions onto nitrocellulose squares and counting the remaining radioactivity after four washes in 100 mL of TBS as described above. For the exchange reaction carried out in the rigorous absence of ADP, removal of ADP from the ATP preparation was accomplished by treatment with the ATP-regenerating system (described above). These reagents converted the small, contaminating amounts of ADP to ATP.

Analysis of Kinetic Data. The substrate concentration dependence of the observed rate constants for CheA phosphorylation and dephosphorylation was analyzed using methods (Matthews & Massey, 1971) originally devised for reactions of the type:

$$A + B \rightleftharpoons C \rightharpoonup D$$

Matthews et al. (1977) previously used such an approach to investigate the three-step, reversible reaction between lipoamide dehydrogenase and its substrate lipoamide. To establish that such an analysis was applicable to the fully reversible, three-step reaction scheme that we propose for CheA phosphorylation/dephosphorylation (see Results), we performed computer simulations of the time courses resulting from this scheme using the kinetic constants determined by first-order analysis of our data. In agreement with the previous work of Matthews et al. (1977), our computer simulations indicated that extrapolation of a double-reciprocal plot (k_{obs}^{-1} versus $[ATP]^{-1}$ or k_{obs}^{-1} versus $[ADP]^{-1}$) to infinite substrate concentration yielded a value for the rate constant governing the phospho-transfer step in the direction being measured

(i.e., k_2 and k_{-2} are the reciprocals of the y-axis intercepts). In addition, the x-axis intercepts of the double-reciprocal plots defined values for $-1/K_d$ for the respective enzyme–substrate complexes. Thus, for our simulations, we set $k_2 = 0.026\ s^{-1}$ (determined from the reciprocal of the y-axis intercept of Figure 1B), $k_{-2} = 0.028\ s^{-1}$ (determined from the reciprocal of the y-axis intercept of Figure 2B), $K_{d,ATP} = 300\ \mu M$ (determined from the reciprocal of the x-axis intercept of Figure 1B), and $K_{d,ADP} = 42\ \mu M$ (determined from the reciprocal of the x-axis intercept of Figure 2B). Although our analysis indicated values for k_2 and k_{-2}, it did not provide specific values for k_1, k_{-1}, k_3, and k_{-3} (which we required for our computer simulations), but rather indicated values for the ratios of k_1/k_{-1} (i.e., $K_{d,ATP}$) and k_{-3}/k_3 (i.e., $K_{d,ADP}$). The actual values of k_1, k_{-1}, k_3, and k_{-3} used in our simulations (see legends for Figures 1 and 2) were calculated from these ratios using the minimum values for k_{-1} and k_{-3} compatible with good fits between the experimental and simulated time courses; when lower values were used for k_{-1} or k_{-3}, it resulted in either (i) a significant lag phase in the simulated time courses which was not evident in the experimental time courses or (ii) a time course that was significantly slower than the experimental one. For simulations performed at a series of ATP and ADP concentrations, we obtained good fits between simulated time courses and experimental data (Figures 1A and 2A), both in terms of the reaction time courses and in terms of the final amount of phospho-CheA at equilibrium.

In simulating the dephosphorylation reaction, we took into account the biphasic nature of the experimental time course. We attributed the biphasic nature of the dephosphorylation reaction to the possibility that phospho-CheA partitions between an ADP-reactive form and an ADP-nonreactive form (representing only 5% of the total phospho-CheA); conversion of the nonreactive to reactive form would account for the slower ADP-independent phase. The simulated time course shown in Figure 2A for phospho-CheA dephosphorylation was obtained by addition of an extra step to our minimal reaction scheme; this additional step was defined by rate constants k_4 and k_{-4}, representing isomerization between the reactive and insensitive forms of phospho-CheA. We used the extent of the slow phase contribution (5%) in defining the initial fraction of phospho-CheA found in the ADP-insensitive form, and the observed rate of the slow phase contribution ($t_{1/2} \approx 500$s) as k_{-4}. k_4 was calculated by assuming partitioning of the phospho-CheA between ADP-nonreactive and -reactive forms to give equilibrium levels of 5% and 95%, respectively.

Kinetic simulations were conducted on a Macintosh SE/30 personal computer using the Stella software package (High Performance Systems, Inc.).

Chromatographic Assay of ATP and ADP Binding by CheA48HQ. The equilibrium chromatography technique of Hummel and Dreyer (1962) was used as previously described (Gegner & Dahlquist, 1991) to investigate the reversible interaction of CheA with ATP and ADP. A sample containing CheA and the ligand of interest was applied to a gel filtration column that had been preequilibrated with the same concentration of ligand as was present in the applied sample. Because the concentration of free ligand in the sample was reduced by the amount bound to CheA, a trough was observed in the elution profile at the expected elution volume for the free ligand. By performing such experiments at a series of ligand concentrations, we were able to determine the mole excess of ligand required to fill the trough and the amount of free and bound ligand at each column concentration of ligand. This involved plotting the area of the trough versus the concentration of ligand in the sample, as described by Gegner and Dahlquist (1991). Samples were pumped through a Superdex 75 HR 10/30 gel filtration column (Pharmacia) at a rate of 0.5 mL/min using a Pharmacia FPLC system at room temperature. The column was equilibrated in 50 mM Tris (pH 7.5)/150 mM KCl/5 mM $MgCl_2$/0.5 mM EDTA/1 mM DTT/0.02% NaN_3 and the indicated ATP or ADP concentration. Samples contained 50 μM CheA48HQ and the appropriate ATP or ADP concentration in 100 μl. The absorbance of the eluant was monitored at 254 or 280 nm.

RESULTS

CheA Autophosphorylation and Dephosphorylation Kinetics. CheA autophosphorylation kinetics were analyzed under pseudo-first-order conditions by incubating purified CheA with varying concentrations of [γ-^{32}P]ATP. At specified times, aliquots were removed, and the reactions were terminated by addition to SDS/PAGE sample-loading buffer. The extent of CheA phosphorylation in each sample was analyzed by SDS/PAGE and liquid scintillation counting. As was previously observed (Hess et al., 1987, 1988b), autophosphorylation of CheA exhibited a simple exponential time course (Figure 1A). Pseudo-first-order rate constants (k_{obs}) were determined from semilogarithmic plots of the reaction time courses (Figure 1A, inset). The pseudo-first-order rate constants exhibited a hyperbolic dependence on the ATP concentration, such that a plot of k_{obs}^{-1} versus $[ATP]^{-1}$ was linear (Figure 1B).

Reactions of phospho-CheA with ADP were initiated by addition of ADP to purified [^{32}P]phospho-CheA, and the kinetics of these reactions were analyzed as above. In contrast to the autophosphorylation time courses, biphasic time courses were observed for the dephosphorylation reaction (Figure 2A). The two kinetic phases were easily resolved: the faster phase (accounting for approximately 95% of the time course) exhibited a rate that increased as the ADP concentration increased; the slower phase proceeded with a $t_{1/2}$ of approximately 500 s, and this value was not affected by the ADP concentration. Because the slower phase made only a very minor contribution to the dephosphorylation time course, we have ignored it in developing the simplest kinetic scheme to account for our data (below). The pseudo-first-order rate constants measured for the faster phase indicated a hyperbolic dependence on the ADP concentration; thus, a double-reciprocal plot of this relationship was linear (Figure 2B) and gave a finite y-axis intercept.

We interpreted our data within the framework of the simplest reaction scheme (Strickland et al., 1975) consistent with the observed kinetic behavior of the forward and reverse reactions:

$$\text{CheA} + \text{ATP} \underset{k_{-1}}{\overset{k_1}{\rightleftharpoons}} \text{CheA·ATP} \underset{k_{-2}}{\overset{k_2}{\rightleftharpoons}} \text{CheA-P·ADP} \underset{k_{-3}}{\overset{k_3}{\rightleftharpoons}} \text{CheA-P} + \text{ADP}$$

For reasons indicated below, we favored this reaction scheme over possible alternatives (Strickland et al., 1975) in which the observed saturation kinetics would have arisen from partitioning of CheA between an ATP-reactive (CheA*) conformation and an ATP-nonreactive conformation (CheA) and from a similar partitioning of phospho-CheA between two conformations, only one of which (CheA-P*) could interact productively with ADP. We observed no evidence of burst phenomena at high ATP or ADP concentrations that would have suggested the existence of CheA* or CheA*-P. Nor did

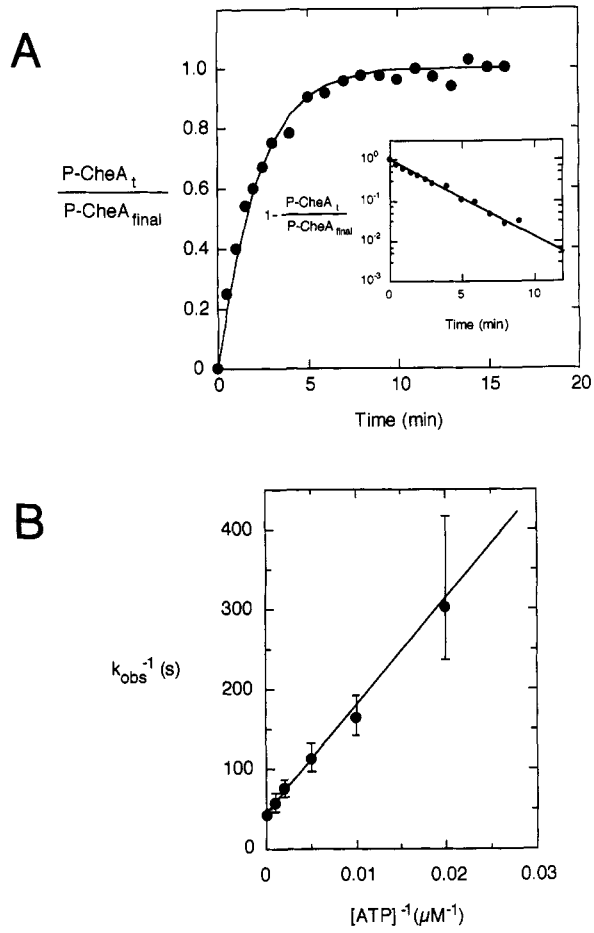

FIGURE 1: Kinetics of CheA autophosphorylation. (A) Typical time course of CheA autophosphorylation. CheA (2 μM final concentration) was incubated with 100 μM [γ-^{32}P]ATP (~6500 cpm/pmol) in TKMD buffer (see Materials and Methods) at 25 °C. Aliquots of the reaction were removed at specific time points and terminated by addition of 2 × SDS/PAGE sample buffer. CheA was separated by SDS/PAGE with simultaneous protein staining using the Chromaphor system (Promega), and CheA bands were excised for scintillation counting. The line through the experimental data points represents a simulated time course for CheA autophosphorylation and was obtained by computer simulation of the time course for the minimal reaction scheme presented under Results using the following specific rate constants: $k_1 = 0.0033\ \mu M^{-1}\ s^{-1}$, $k_{-1} = 1\ s^{-1}$, $k_2 = 0.026\ s^{-1}$, $k_{-2} = 0.028\ s^{-1}$, $k_3 = 0.2\ s^{-1}$, and $k_{-3} = 0.0048\ \mu M^{-1}\ s^{-1}$. Values for k_2 and k_{-2} were assigned based on analysis of data presented in Figures 1 and 2. The values used for k_1, k_{-1}, k_3, and k_{-3} in this simulation should be viewed as lower limits in that they represent the minimal rate constants that resulted in simulated time courses that corresponded well with the experimental time courses (e.g., lacking a noticeable lag phase and indicating the same $t_{1/2}$ to within 20%); the real values for k_1, k_{-1}, k_3, and k_{-3} may be considerably larger than these estimates. A semilogarithmic plot of the experimentally determined time course is shown in the inset. (B) Double-reciprocal plot of the observed pseudo-first-order rate constant (k_{obs}) for CheA autophosphorylation versus ATP concentration. Error bars represent the standard errors of the mean.

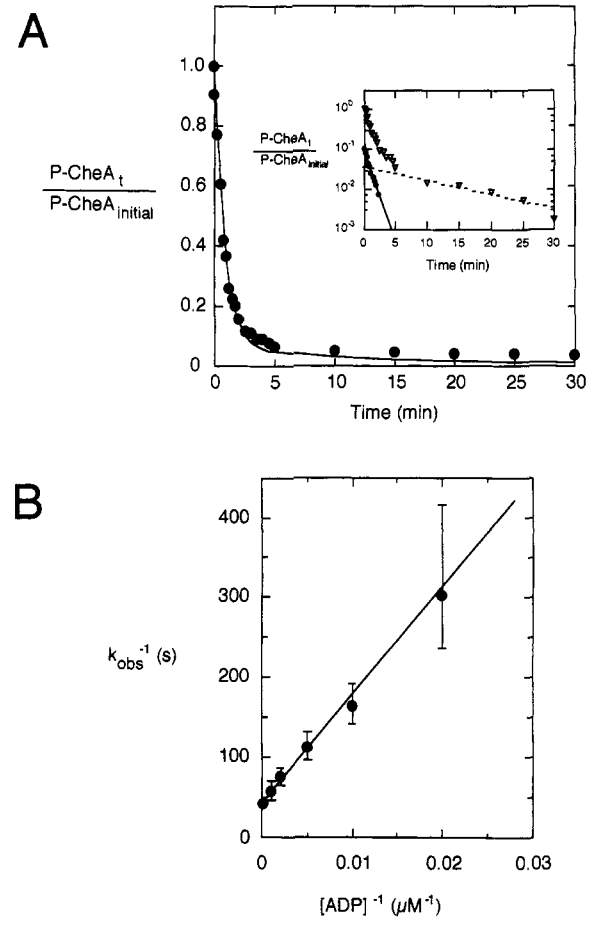

FIGURE 2: Kinetics of phospho-CheA dephosphorylation. (A) Typical time course of phospho-CheA dephosphorylation by ADP. Purified [^{32}P]phospho-CheA (1 μM final concentration, ~2500 cpm/pmol) was incubated with 100 μM ADP in TKMD buffer at 25 °C. The reaction was analyzed as described in Figure 1. A simulated time course of the phospho-CheA dephosphorylation reaction is shown as the line drawn through the experimental data points and was obtained by computer simulation (using parameters described in the legend of Figure 1, except that an extra step defined by the rate constants $k_4 = 0.000074\ s^{-1}$ and $k_{-4} = 0.0014\ s^{-1}$ was added to take into account the biphasic nature of the dephosphorylation reaction as described under Materials and Methods). Inset: A semilogarithmic plot for the experimental time course shows the biphasic nature of the dephosphorylation time course (open triangles). The dashed line shows the rate and extent of contribution of the slow phase, whereas the solid line (closed circles) shows the fast phase contribution (shown shifted down by a magnitude for the sake of clarity) after subtraction of the slow phase contribution. (B) Double-reciprocal plot of the observed pseudo-first-order rate constant (k_{obs}) for phospho-CheA dephosphorylation versus ADP concentration. Error bars represent the standard errors of the mean.

we observe such burst kinetics for the forward reaction at a series of different pHs and temperatures (Tawa, Huang, and Stewart, unpublished results). Although such negative evidence is hardly compelling, in the absence of any evidence supporting the existence of a CheA* species, we chose to interpret our data within the framework of the reaction specified above, one that applies to a large number of enzymes (Strickland et al., 1975). Further support for this mechanism is found in the agreement between our kinetically determined K_d values and those determined independently in ligand binding experiments (see below).

To extract information about rate constants for specific steps of this reaction scheme, we analyzed the data for the forward and reverse reactions (Figures 1B and 2B) using computer simulations and methods described previously (Matthews & Massey, 1971) as detailed under Materials and Methods. Analysis of the experimental results presented in Figures 1B and 2B enabled us to assign values to several of the rate constants and binding equilibria defined in the reaction scheme specified above. These values are summarized in Table 1.

Binding of ATP and ADP to CheA. To further investigate the binding interaction between CheA and its ligands ATP and ADP, we used the equilibrium chromatography method of Hummel and Dreyer (1962), as previously described for analysis of the binding interaction between the CheA and CheW proteins (Gegner & Dahlquist, 1991). We performed

Table 1: Kinetic Constants for CheA Interaction with ATP and ADP[a]

constant	value
$K_{d,ATP} = k_{-1}/k_1$	300 ± 75 μM
k_2	0.026 ± 0.004 s^{-1}
k_{-2}	0.028 ± 0.003 s^{-1}
$K_{d,ADP} = k_3/k_{-3}$	42 ± 8 μM

[a] Values were determined as described under Results and under Materials and Methods and refer to kinetic constants for the minimal reaction scheme discussed under Results. ± values indicate standard errors of the mean of at least three independent determinations.

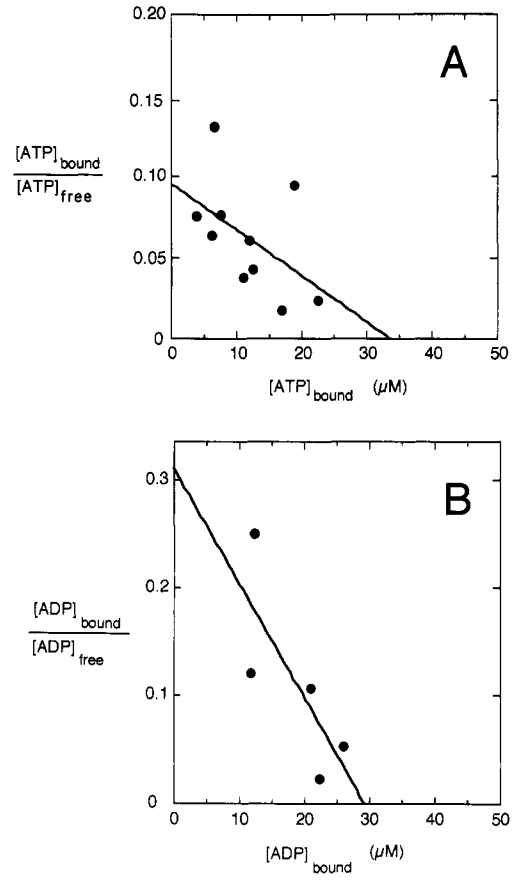

FIGURE 3: Scatchard plots describing binding of ATP and ADP to CheA. The chromatography technique of Hummel and Dreyer (1962) was used to obtain these data as described by Gegner and Dahlquist (1991). The ratio of bound to free ATP (or ADP) was determined and plotted against the bound concentration for data obtained at a series of concentrations of free ligand. CheA48HQ, a CheA mutant lacking the autophosphorylation site, was used in these experiments to overcome complications arising from an active enzymatic activity. Experiments were performed with column concentrations (free ligand concentrations) of 50, 100, 200, 300, and 1000 μM ATP and 50, 100, 200, 500, and 1000 μM ADP.

these experiments with CheA48HQ, a CheA mutant lacking the site of autophosphorylation but presumably retaining an intact binding site. Several different column concentrations of ATP or ADP were used to obtain a quantitative description of binding interactions between CheA and ATP or ADP. From the slopes of Scatchard plots of these data (Figure 3), we determined K_d values of 350 ± 150 μM for the CheA48HQ·ATP complex and 95 ± 60 μM for the CheA48HQ·ADP complex. These values are in reasonable agreement with our kinetically determined $K_{d,ATP}$ of 300 μM and the previously determined value for $K_{i,ADP}$ of 70 μM [Borkovich & Simon, 1990; cited in Bourret et al. (1991)]. The somewhat lower $K_{d,ADP}$ that we determined from the dephosphorylation kinetics (42 μM) may have resulted from the influence of the

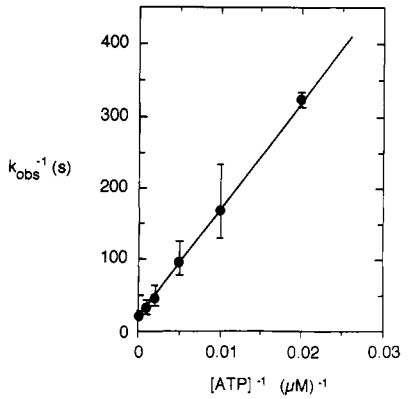

FIGURE 4: Steady-state kinetics of CheA autophosphorylation. A coupled ATPase assay was used as described under Materials and Methods to measure the ATP dependence of CheA's autophosphorylation activity in the presence of CheY and CheZ under steady-state conditions. Data are presented as a double-reciprocal plot of the observed velocity of ATP turnover versus ATP concentration. Error bars represent the standard errors of the mean.

phosphoryl group on the properties of CheA. The x-axis intercepts of the Scatchard plots indicate a binding stoichiometry of 0.6–0.7 ATP or ADP bound per CheA molecule.

Kinetics of CheA Autophosphorylation under Steady-State Conditions. In addition to the single-turnover kinetics described above, we also investigated CheA's autophosphorylation reaction under multiple-turnover conditions that would more closely approximate those found intracellularly. A coupled ATPase assay was utilized to measure the ATP dependence of CheA's kinase activity under steady-state conditions in the presence of CheY and CheZ. The presence of excess CheY and CheZ caused rapid dephosphorylation of CheA, enabling CheA to undergo further rounds of autophosphorylation, while the presence of the coupling system components (PEP, NADH, pyruvate kinase, lactate dehydrogenase) converted the ADP generated by CheA back to ATP at the expense of PEP dephosphorylation and NADH oxidation (Norby, 1988; Lukat et al., 1991; Ninfa et al., 1991). Consistent with the single-turnover work, the steady-state rates of CheA autophosphorylation measured over a range of ATP concentrations exhibited a hyperbolic dependence on ATP concentration (Figure 4). The K_M of CheA for ATP under these steady-state conditions was 770 μM; this value is not necessarily directly comparable to the K_d determined in the single-turnover experiments because under steady-state conditions the value of K_M for the reaction scheme presented above may be affected not only by k_1 and k_{-1} but also by rate constants for subsequent steps. The V_{max} in the steady-state experiment indicates a limiting rate constant of approximately 0.05 s^{-1}, which is almost 2-fold faster than the value determined in the single-turnover experiments. High-affinity CheA·CheY complexes (Schuster et al., 1993) have been demonstrated recently, and so the enhanced rate of CheA autophosphorylation we observed in the steady-state experiments may reflect the kinetic properties of CheA in such a complex.

Kinetics of CheA48HQ/CheA470GK Heterodimer Trans-Autophosphorylation. The kinase-deficient mutant CheA48HQ contains a glutamine in place of histidine-48, the autophosphorylation site of CheA (Hess et al., 1988a). The CheA470GK variant (Swanson et al., 1993a) contains a substitution at one of a number of glycine residues that may comprise a glycine-rich nucleotide binding region (Stock et al., 1989; Parkinson & Kofoid, 1992). Although both of these mutants lack the ability to autophosphorylate individually, "autophosphorylation" activity is reestablished when they are

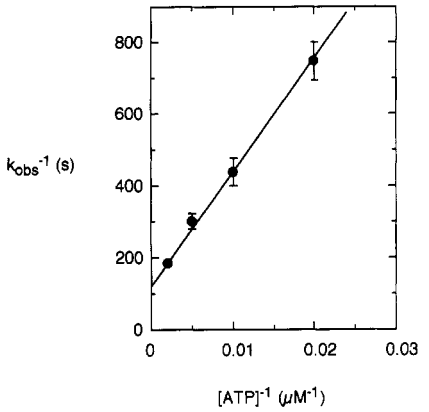

FIGURE 5: Kinetics of trans-phosphorylation for CheA48HQ/CheA470GK heterodimers. A double-reciprocal plot of the observed pseudo-first-order rate constant for the trans-phosphorylation reaction between CheA48HQ and CheA470GK versus ATP concentration is shown. Reactions were monitored at 50, 100, 200, and 500 μM ATP after allowing 60-min equilibration between 2 μM CheA48HQ and CheA470GK as described under Materials and Methods. Error bars represent the standard errors of the mean.

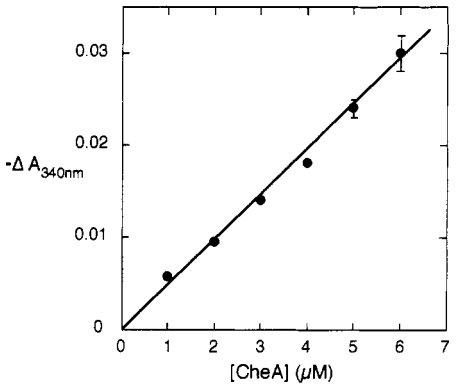

FIGURE 6: Extent of CheA phosphorylation measured by NADH oxidation. CheA aliquots (500 pmol) were added to a preequilibrated reaction mixture (500 μL) containing 2 mM ATP and the ATP-regenerating system as described under Materials and Methods. NADH levels were measured spectrophotometrically at 340 nm ($\epsilon_{NADH \rightarrow NAD^+} = 0.0062\ \mu M^{-1}cm^{-1}$). The decrease in A_{340} was recorded after successive addition of each CheA aliquot. Error bars represent the standard errors of the mean.

combined. This appears to result from formation of CheA48HQ/CheA470GK heterodimers in which phosphorylation of His-48 on CheA470GK is catalyzed by the intact kinase activity of CheA48HQ (Swanson et al., 1993a).

To investigate the kinetics of this trans-autophosphorylation reaction, we analyzed the reaction in a fashion analogous to that described above for the wild-type protein. At a series of ATP concentrations, each time course of the trans-autophosphorylation reaction could be fit to a single exponential, as was observed for wild-type CheA. A double-reciprocal plot of the observed pseudo-first-order rate constant for trans-autophosphorylation versus ATP concentration is shown in Figure 5. These data demonstrate saturation kinetics and indicate a K_d of approximately 240 μM for the complex of ATP with the CheA48HQ/CheA470GK heterodimer and a $k_{limiting}$ of approximately 0.008 s^{-1}, a value that is somewhat slower than that determined for autophosphorylation of wild-type CheA heterodimers ($k_{limiting} = 0.026 s^{-1}$). The slower rate of phosphorylation obtained with the heterodimer therefore appears to result from a decrease in k_2 (the rate constant governing the phospho-transfer step) whereas the affinity of the heterodimer for ATP is approximately the same as that exhibited by the wild-type CheA homodimer. It is conceivable that the decrease in k_2 is due to elimination of *cis* phosphorylation (i.e., intraprotomer) in the mutant heterodimers. Alternatively, it is also quite possible that autophosphorylation of the wild-type protein occurs primarily or exclusively via trans-phosphorylation but that the mutations (H48Q and/or G470K) affect CheA structure in a way that slows this process.

Stoichiometry of CheA Phosphorylation. The number of phosphorylation sites on CheA is an important value when considering the molecular details of CheA autophosphorylation. Previous work indicates that autophosphorylation occurs within and not between dimers (Hess et al., 1988b; Swanson et al., 1993a) and that this activity may result from trans-phosphorylation of one CheA subunit by the other subunit (Swanson et al., 1993a; Wolfe & Stewart, 1993). Both subunits would potentially act as substrates in trans-phosphorylation reactions by the opposite subunit. The phosphorylation stoichiometry of 0.7:1 phosphate per CheA monomer reported by Hess et al. (1987) is consistent with the idea that histidine-48 from each subunit can be phosphorylated, but does not rule out a lower stoichiometry. To more rigorously address this question, we utilized a coupled ATPase assay to estimate the amount of ADP generated when CheA autophosphorylates in the presence of saturating ATP. In this assay, known amounts of CheA were added to a preequilibrated reaction mixture containing ATP, NADH, phosphoenolpyruvate, pyruvate kinase, and lactate dehydrogenase. Because the ATP concentration was very high (2 mM), when an aliquot of CheA was added, CheA autophosphorylation proceeded to completion, and the ADP generated resulted in an equivalent amount of NADH oxidation which was measured spectrophotometrically. The decrease in absorbance at 340 nm therefore enabled estimation of the stoichiometry of ADP molecules generated per CheA molecule. Using this assay, we detected a decrease of approximately 0.005 absorbance unit per micromolar CheA addition (Figure 6). Taking into account the fact that our purified CheA preparation consisted of approximately 10% $CheA_S$ (as determined by Coomassie blue staining), the observed absorbance changes indicated a phosphorylation stoichiometry of approximately 0.9:1. The result of this assay was verified using a radiolabeling assay (data not shown).

CheA-Phosphate/ATP Exchange. Borkovich and Simon (1990) reported the lability of [^{32}P]phospho-CheA after addition of excess unlabeled ATP in pulse–chase experiments. This dephosphorylation was attributed to the ability of phospho-CheA to exchange covalently bound phosphate with ATP. Because we would want to include such an exchange reaction in our reaction scheme, we further investigated the nature and kinetics of ^{32}P exchange between phospho-CheA and unlabeled ATP. We examined the possibility that the loss of label from phospho-CheA on addition of excess cold ATP was due to dephosphorylation of CheA by contaminating ADP present in the ATP preparations. Addition of unlabeled, "high purity" ATP resulted in a steady loss of label from CheA-phosphate over a 1 h period (Figure 7), consistent with the observations of Borkovich and Simon (1990). However, this loss of ^{32}P label from phospho-CheA was eliminated when the cold ATP was first treated with an ATP-regenerating system to remove traces of ADP (Figure 7). The small initial drop in the level of [^{32}P]phospho-CheA may have been due to small quantities of ADP evolved as a result of autophosphorylation of unphosphorylated CheA dimers present in the initial reaction mixture. Thus, the lability of phospho-CheA observed after addition of ATP was not due to a phosphoryl group exchange reaction, but rather due to dephosphorylation

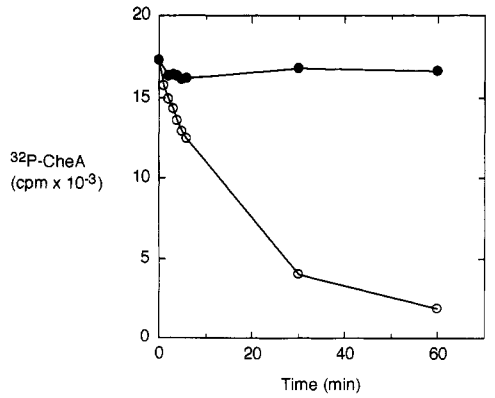

FIGURE 7: Phospho-CheA dephosphorylation upon addition of ATP. The amount of [^{32}P]phospho-CheA (2 μM final concentration) was monitored after adding excess unlabeled ATP (open circles) or unlabeled ATP that had been pretreated with an ATP-regenerating system to rigorously remove trace amounts of contaminating ADP (closed circles). In both cases, the final ATP concentration was 1 mM.

of CheA-phosphate by small quantities of ADP, commonly found in ATP preparations, that became significant when large amounts of ATP were added.

DISCUSSION

CheA is thought to be capable of adopting three distinct forms *in vivo* (Borkovich & Simon; 1990): (i) a "closed" form of CheA exists as a soluble cytoplasmic fraction with low specific activity; (ii) an "open" or activated form of CheA results from association of CheA with receptor proteins and CheW; and (iii) a "sequestered" form is generated when CheA is coupled to a receptor to which chemoattractant has bound. In this study, we focused on the *in vitro* kinetic properties of the "closed" form of CheA. A minimal kinetic model was developed describing both autophosphorylation and dephosphorylation reactions. In both the forward and reverse reactions, saturation kinetics were observed, consistent with the formation of CheA·ATP and P-CheA·ADP complexes prior to phospho-transfer. The kinetically defined K_d of the CheA·ATP complex was determined to be approximately 300 μM, and a limiting rate constant for autophosphorylation was estimated to be 0.026 s^{-1}. These kinetic parameters are equivalent to those previously reported for the *Salmonella typhimurium* CheA protein (Wylie et al., 1988), based on analysis of initial rate data obtained under somewhat different conditions. We detected a maximum level of CheA phosphorylation of 0.9:1 phosphate to CheA, suggesting that each CheA protomer within a dimer is capable of being phosphorylated. When phosphorylated, CheA readily dephosphorylates in the presence of ADP. The K_d of the phospho-CheA·ADP complex is approximately 42 μM, and the extrapolated limiting rate constant for dephosphorylation is 0.028 s^{-1}. We also established that phospho-CheA does not readily exchange phosphate with ATP.

Our characterization of the kinetic properties of the "closed" or "uncoupled" form of CheA provides a kinetic framework that will be useful for analyzing the effects of coupling CheA to the MCPs and for interpreting the effects of various mutations. While such work is currently underway, it is informative to speculate at this time about the nature of CheA regulation in the ternary complexes CheA·CheW·MCP. Since physiological concentrations of ATP and ADP are 3000 and 250 μM, respectively (Bochner & Ames, 1982), our kinetic results suggest that it is unlikely that regulation of CheA autokinase activity involves changes of the affinity of CheA for ATP or ADP. For example, it would not be possible to accelerate the autophosphorylation by increasing the affinity of CheA for ATP (i.e., decreasing $K_{d,ATP}$). Therefore, it appears likely that MCP-mediated regulation of CheA involves changes of CheA's intrinsic reactivity with ATP (k_2 in our scheme), and it is likely that this step is rate-limiting in the pathway to generate phospho-CheY (Ninfa et al., 1991).

Any model describing how phospho-CheY levels are regulated must also account for the antagonistic activity of CheZ, a protein that markedly accelerates CheY dephosphorylation (Hess et al., 1988b,c) but which has not, as yet, been demonstrated to be subject to regulation. The intracellular level of phospho-CheY reflects the relative rates of CheY phosphorylation and dephosphorylation by CheA and CheZ, respectively. *In vitro,* autodephosphorylation of phospho-CheY proceeds with a first-order rate constant of approximately 0.04 s^{-1}. This rate is accelerated markedly by even low levels of CheZ; for example, in the presence of 0.02 μM CheZ, 8 μM phospho-CheY was hydrolyzed with a first-order rate constant of 0.1 s^{-1} (Huang & Stewart, 1993). With CheZ concentrations closer to the physiological level of 20 μM (Matsumura et al., 1990; Kuo & Koshland, 1987), we would predict rates of CheZ-mediated hydrolysis of phospho-CheY to be considerably faster, perhaps even as fast as ~45 s^{-1} (this estimate assumes that the rate of CheY dephosphorylation has a linear dependence on the CheZ concentration, although we have no data to support this assumption). How fast could we expect generation of phospho-CheY to be? Previous work (Hess et al., 1988b; Lukat et al., 1991) has demonstrated that phospho-transfer from phospho-CheA to CheY is very rapid. Therefore, the rate-limiting step in the production of phospho-CheY is expected to be CheA autophosphorylation. The maximal rate of autophosphorylation is quite slow ($k_{limiting}$ ~ 0.026 s^{-1}) for uncoupled CheA relative to the rate expected for CheY dephosphorylation, such that essentially no phospho-CheY would accumulate as a consequence of the activity of the "closed" CheA. To enable production of a significant steady-state level of phospho-CheY (e.g., a few percent of the total CheY pool), the rate of CheA autophosphorylation would have to increase substantially to ~5 s^{-1}. Rigorous kinetic analyses are currently under way in our laboratory to determine the maximum rate of CheA autophosphorylation when coupled to the transducer/receptor proteins; however, a rough estimate may be obtained by comparing the kinetics of CheY phosphorylation mediated by the receptor-coupled and -uncoupled forms of CheA. Coupling of CheA to Tar has been shown to result in a 300-fold increase in the level of CheY-phosphate within a 10-s time period (compared to the amount of phospho-CheY generated by uncoupled CheA; Borkovich et al., 1989). A 300-fold enhancement in CheA's kinase activity at saturating ATP concentrations would enable CheA autophosphorylation to proceed with a rate constant of approximately 8 s^{-1}, a rate that would enable the steady-state level of phospho-CheY to reach 3–5% of the total CheY pool. This estimate assumes that CheA autophosphorylation is rate-limiting in generating phospho-CheY and that the concentrations of CheA, CheW, transducer, CheY, and CheZ are in the range tabulated by Bray et al. (1993).

ACKNOWLEDGMENT

We gratefully acknowledge Dr. J. S. Parkinson for providing *E. coli* strains, members of the R. A. Murgita laboratory for

FPLC instrument time and assistance, and Drs. K. Clark and B. Bourret for comments on the manuscript.

REFERENCES

Barak, R., & Eisenbach, M. (1992) *Biochemistry 31*, 1821–1826.

Bochner, B. R., & Ames, B. N. (1982) *J. Biol. Chem. 257*, 9759–9769.

Borkovich, K. A., & Simon, M. I. (1990) *Cell 63*, 1339–1348.

Borkovich, K. A., Kaplan, N., Hess, J. F., & Simon, M. I. (1989) *Proc. Natl. Acad. Sci. U.S.A. 86*, 1208–1212.

Bourret, R. B., Hess, J. F., & Simon, M. I. (1990) *Proc. Natl. Acad. Sci. U.S.A. 87*, 41–45.

Bourret, R. B., Borkovich, K. A., & Simon, M. I. (1991) *Annu. Rev. Biochem. 60*, 401–441.

Bray, D., Bourret, R. B., & Simon, M. I. (1993) *Mol. Biol. Cell 4*, 469–482.

Gegner, J. A., & Dahlquist, F. W. (1991) *Proc. Natl. Acad. Sci. U.S.A. 88*, 750–754.

Gegner, J. A., Graham, D. R., Roth, A. F., & Dahlquist, F. W. (1992) *Cell 70*, 975–982.

Hess, J. F., Oosawa, K., Matsumura, P., & Simon, M. I. (1987) *Proc. Natl. Acad. Sci. U.S.A. 84*, 7609–7613.

Hess, J. F., Bourret, R. B., & Simon, M. I. (1988a) *Nature 336*, 138–143.

Hess, J. F., Oosawa, K., Kaplan, N., & Simon, M. I. (1988b) *Cell 53*, 79–87.

Hess, J. F., Bourret, R. B., Oosawa, K., Matsumura, P., & Simon, M. I. (1988c) *Cold Spring Harbor Symp. Quant. Biol. 53*, 41–48.

Huang, C., & Stewart, R. C. (1993) *Biochim. Biophys. Acta 1202*, 297–304.

Hummel, J. P., & Dreyer, W. J. (1962) *Biochim. Biophys. Acta 63*, 530–532.

Kuo, S. C., & Koshland, D. E., Jr. (1987) *J. Bacteriol. 169*, 1307–1314.

Liu, J., & Parkinson, J. S. (1991) *J. Bacteriol. 173*, 4941–4951.

Lukat, G. S., Lee, B. H., Mottonen, J. M., Stock, A. M., & Stock, J. B. (1991) *J. Biol. Chem. 266*, 8348–8354.

Lupas, A., & Stock, J. (1989) *J. Biol. Chem. 264*, 17337–17342.

Matsumura, P., Roman, S., Volz, K., & McNally, D. (1990) in *Biology of the Chemotactic Response* (Armitage, J. P., & Lackie, J. M., Eds.) pp 135–154, Cambridge University Press, Cambridge, U.K.

Matthews, R., & Massey, V. (1971) in *Flavins and Flavoproteins* (Kamin, H., Ed.) pp 329–348, University Park Press, Baltimore.

Matthews, R. G., Ballou, D. P., Thorpe, C., & Williams, C. H., Jr. (1977) *J. Biol. Chem. 252*, 3199–3207.

McNally, D. F., & Matsumura, P. (1991) *Proc. Natl. Acad. Sci. U.S.A. 88*, 6269–6273.

Ninfa, E. G., Stock, A., Mowbray, S., & Stock, J. (1991) *J. Biol. Chem. 266*, 9764–9770.

Norby, J. G. (1988) *Methods Enzymol. 156*, 116–119.

Parkinson, J. S. (1993) *Cell 73*, 857–871.

Parkinson, J. S., & Kofoid, E. (1992) *Annu. Rev. Genet. 26*, 71–112.

Roman, S. J., Meyers, M., Voltz, K., & Matsumura, P. (1992) *J. Bacteriol. 171*, 3609–3618.

Schuster, S. C., Swanson, R. V., Alex, L. A., Bourret, R. B., & Simon, M. I. (1993) *Nature 365*, 342–347.

Stewart, R. C., & Dahlquist, F. W. (1987) *Chem. Rev. 87*, 997–1025.

Stewart, R. C., Roth, A. F., & Dahlquist, F. W. (1990) *J. Bacteriol. 172*, 3388–3399.

Stock, J. B., Ninfa, A. J., & Stock, A. M. (1989) *Microbiol. Rev. 53*, 450–490.

Strickland, S., Graham, P., & Massey, V. (1975) *J. Biol. Chem. 250*, 4048–4052.

Swanson, R. V., Bourret, R. B., & Simon, M. I. (1993a) *Mol. Microbiol. 8*, 435–441.

Swanson, R. V., Schuster, S. C., & Simon, M. I. (1993b) *Biochemistry 32*, 7623–7629.

Wolfe, A. J., & Stewart, R. C. (1993) *Proc. Natl. Acad. Sci. U.S.A. 90*, 1518–1522.

Wylie, D., Stock, A., Wong, C.-Y., & Stock, J. (1988) *Biochem. Biophys. Res. Comm. 151*, 891–896.